Research Article

Enhanced solubility and dissolution rate of raloxifene using cycloencapsulation technique

Abstract

The aim of this study was to improve the water solubility of raloxifene by complexing it with sulphobutylether-β-cyclodextrin. Inclusion complexation in aqueous solution and solid state was evaluated by the phase solubility diagram, powder X-ray diffractometer, Fourier-transform infrared spectroscopy, nuclear magnetic resonance, scanning electron microscopy, hot stage microscopy and transmission electron microscopy. The inclusion complex behavior of raloxifene and sulphobutylether-β-cyclodextrin were examined by molecular modeling method. The phase solubility diagram with sulphobutylether-β-cyclodextrin was classified as AL-type curve, indicating the formation of 1:1 stochiomatric inclusion complex. The apparent solubility constants calculated from phase solubility diagram was 753 M^{-1}. Aqueous solubility and dissolution studies indicated that the dissolution rates were remarkably increased in inclusion complex, compared with the physical mixture and drug alone. In conclusion, inclusion complexation with sulphobutylether-β-cyclodextrin is an easy approach to increase raloxifene solubility and dissolution rate which could have implications in its bioavailability considering it a Biopharmaceutical Classification System Class II drug.

Keywords: raloxifene, sulphobutylether-β-cyclodextrin, hot stage microscopy, phase solubility, dissolution rate, molecular modeling

Elsavath Puramdas, Charan Singh, Vivek Kumar, Tara Datt Bhatt, Sabyasachi Roy, Masilamani Elizabeth Sobhia, Manjinder Singh Gill, Sarasija Suresh
Department of Obstetrics & Gynecology, North Eastern Indira Gandhi Regional Institute of Health & Medical Sciences (NEIGRIHMS), India

Correspondence: Sarasija Suresh, Department of Pharmaceutical Technology (Formulation), National Institute of Pharmaceutical Education and Research (NIPER), Sector 67, S.A.S. Nagar (Mohali) Punjab- 160062, India, Tel +91 8762002557, Email sarasija_shotmail.com

Introduction

The main rate limiting step in the absorption of poorly soluble drugs across biological barriers is its dissolution rate. All the new chemical entities (~70%) entering into the drug discovery programme do not exhibit sufficiently solubility in the physiological media to allow consistent gastrointestinal absorption of high order of magnitude required for further therapeutic activities. The solubility of a drug in the GI tract is governed by multiple factors and is inherently a complex phenomenon often resulting in erratic absorption of poorly soluble drugs. Therefore, it is important to introduce effective methods to enhance the solubility and dissolution rate of the drug aiming to improve its bioavailability, increase the predictability of the response and/or reduce the dose. To overcome these problems, various approaches have been developed, such as pro-drugs, addition of surfactants, salt selection, particle size reduction, solid dispersion[1–3] inclusion complexes with cyclodextrins and phospholipid complex.[4–6] Complexation with cyclodextrins (CDs) has been widely used to enhance the bioavailability of poorly soluble drugs by increasing the drug solubility, dissolution and/or permeability.[6–15]

Raloxifene (RAL) belongs to benzothiophene class of compounds and is a BCS class II drug with poor solubility (0.25 mg/L) and high permeability. Owing to the poor solubility and high first pass metabolism, RAL absolute oral bioavailability is only 2%.[16] The most widely used natural cyclodextrin, β-CD, is limited in its pharmaceutical applications due to its limited aqueous solubility (1.85g/100ml). Therefore, chemically modified β-CDs have been synthesized to overcome this problem. Examples include heptakis-(2, 6-O-dimethyl) (DM-β-CD), hydroxypropyl-β-CD (HP-β-CD) and sulphobutylether-β-CD (SBECD).[17,18]

Literature lacks any data about the effect of RAL-SBECD complexation to enhance the solubility and dissolution rate. RAL-SBECD inclusion complexation was investigated to evaluate its impact on solubility of RAL. We confirmed the stoichiometry of RAL

and SBECD by phase solubility. Characterization of complex and its evaluation was by XRD, FTIR, SEM, HSM and TEM analysis. We evaluated the solubilization effect of SBECD on RAL by *in vitro* release study. An attempt was made to investigate the host-guest interaction by *in silico* molecular modeling studies, which essentially involve determining the ease which RAL can be docked within the CD molecule.

Materials and methods

Chemicals

RAL was obtained as a gift sample from Wuhan Better Organic Pvt. Ltd. China. SBECD was obtained as a kind gift sample from Cydex Pharmaceuticals.USA. All other solvents used in the study were of analytical grade and used as such.

Preparation of raloxifene-SBECD complex

RAL-SBECD complex was prepared by freeze drying. Briefly, RAL and SBECD were dissolved in alcoholic aqueous solution under constant stirring and were freeze dried (Virtis advantage, 2.0 EL Bench Top freeze drier, USA) at -20°C for 24 h to obtain the final complex as a solid dispersion. In addition, we prepared a physical mixture of RAL with SBECD by dispersing individual components at 1:1 molar ratio.

Standard curve of raloxifene

A standard curve was prepared by dissolving RAL in methanol (0.1-100µg/ml) and estimating by HPLC (Shimadzu, Japan) at 287nm. The equation obtained was A = 76950C + 1762 (R2 = 0.999).[16]

Determination of raloxifene in SBECD complex

The drug content was determined by dissolving 10 mg of the complex in 10 ml of methanol and analyzing an aliquot (20µl) by HPLC at 287 nm. Phenomenex C18 column (250mm×4.6mm, 5m),

was selected as the stationary phase, which was operated at room temperature. The mobile phase consisted of ACN: Phosphate buffer (10mM) in the 64:36 proportions. The flow rate was maintained at 1ml/min. The percentage yield was calculated as follows:

$$\text{Percentage yield} = \frac{\text{Practical yield}}{\text{Theoritical yield}} \times 100 \qquad (1)$$

Phase solubility study

The stoichiometry of RAL and SBECD was determined by phase solubility study by the method described by Higuchi and Connors.[19] Briefly, an excess RAL was added to 15ml glass vials containing SBECD at concentration ranging from 1 to 20mM. The mixtures were shaken in shaker water bath for 24 h at $37\pm5°C$. After equilibrium was attained, samples were filtered through 0.45 membrane filter and analyzed by HPLC at 26=87nm. The phase solubility profiles were obtained by plotting solubility of RAL vs. concentrations of SBECD. The apparent stability constant, K_C, of the RAL and SBECD complex is calculated from the slope and the intercept of the linear segment of the phase solubility line by:

$$\text{Stability constant}(Kc) = \frac{k}{S_0(1-k)} \qquad (2)$$

Where S_0 is the solubility of the drug in the absence of cyclodextrin, and k is the slope of the straight line. The study was conducted in triplicate.

Molecular docking study

The GOLD program[20] employed for computational studies to verify the structure of the RAL and SBECD complex. The initial coordinates of the β-CD were taken from the crystal structure, 2ZYN. It has a bucket shape with crystal structure resolution of 1.70 Å.[21] It is substituted with four sulphobutyl ether group at the top side and by three groups at the rear side of the β-CD bucket. It is further submitted to aggregate constraint minimization by Sybyl7.1 installed on a silicon graphics fuel work station. The conjugate gradient method with Tripos force field with 0.05 kcal/mol energy gradient convergence criterion was adopted as the minimization parameter. The RAL molecule was docked into the obtained SBECD structure to form a complex by the GOLD program. The obtained complex is further submitted to geometry optimization by the b3lyp method with 6-31+g(d) basis set using Gaussian-03.[22] The energy of complex was calculated corresponding to the molecular form of SBECD, RAL and their docked complex by the following equation:

$$E_{\text{complex}} = E_{\text{docked\_complex}} - \left(E_{\text{raloxifene}} + E_{\text{sulpobutyl ether - cyclodextrain}} \right) \qquad (3)$$

Here,

E_{complex} = Energy of complex formation

$E_{\text{docked\_complex}}$ = Energy of docked complex

$E_{\text{reloxifene}}$ = Energy of raloxifene

$E_{\text{cyclodextrin}}$ = Energy of sulphobutyl ether-β- cyclodextrin

Characterization

FTIR: FTIR was employed for preliminary characterization of RAL-SBECD complex. Spectra of RAL, SBECD, physical mixture and RAL-SBECD complex were recorded on a FTIR spectrophotometer (Nicolet, Impact 410, USA) equipped with a deuterated triglycine

sulfate detector. Potassium bromide pellet method was employed, and background spectrum was collected under identical conditions. Each spectrum was derived from averaged scans collected in the region 400–4000 cm^{-1} at a spectral resolution of 2cm^{-1}, Fourier transformed and ratioed against background interferogram. Spectra obtained were analyzed with Omnic 5.1a software (Thermo Nicolet, USA).

PXRD: Powder X-ray diffraction patterns were recorded with D8 advanced (Bruker Germany) using Ni-filtered Cu Kα (1.542 A°) radiation (40 kV, 40am) for RAL, RAL-SBECD complex and physical mixture. Samples were mounted on the sample holder and scanned from 4° to 40° in 2θ at a speed of 0.01°/min.

SEM: The surface morphology of RAL, SBECD, physical mixture and RAL-SBECD complex were examined by SEM (Hitachi S-3400 N, Japan). Samples were prepared by affixing powder samples on to a double-sided adhesive tape pasted over sample stubs and sputter coated with gold using ion sputter E-1010, Hitachi under vacuum of 1-10 Pascal. The samples were scanned with an electron beam of acceleration potential of 1.2 kV and images were collected at different magnifications.

TEM: The morphological structures of drug encapsulated RAL-SBECD complex investigated by TEM using TECNAI G4 microscope with an accelerating voltage of 200 kV, for the TEM analysis carbon coated copper TEM grids (200 mesh) were employed.

HSM: The change in crystal behavior of RAL after complex formation was investigated by hot stage microscopy (Leitz 1350, Leica, Germany) under the light microscope (Leica, Germany) equipped with a 35-mm camera (Leica MPS 52). The sample was placed over a drop of silicone oil, covered with a cover slip and heated at a rate of 10°C/min during the study.

NMR: Proton NMR spectra of RAL, RAL-SBECD complex, and SBECD was recorded by an Avance (AV III) 400 MHz 2.1 Topspin (USA) software at 400 MHz to analyse the chemistry of complex. In reference employed was tetramethyl silane.

Determination of solubility: The solubility of RAL and RAL-SBECD complex was individually determined in water. Briefly, added an excess amount of RAL to 5 ml of distilled water and stirred in a shaker water bath for 24 h at $37\pm1°C$. Subsequently, the suspension was centrifuged, supernatant filtered through a 0.45 μm membrane filter and analyzed by HPLC system (Shimadzu, Japan) at 287 nm. All experiments were performed in triplicate.

In vitro release studies

The dissolution behavior of pure RAL, physical mixture and RAL-SBECD complex was studied in Electro lab TDT 08L Dissolution tester (USP) type II apparatus. The medium consisted of 900 ml of phosphate buffer pH 6.8 maintained at 37±0.5°C. A sample equivalent to 20 mg RAL was taken for the study. Five ml aliquots were collected at different time intervals of 0.25, 0.5, 1, 2, 3, 4, 5 h and filtered through 0.45 micron polycarbonate filter and analyzed by HPLC. Additionally, the dissolution efficiency (DE) was studied for 5 h (DE$_{5h}$,), calculated from the area under the dissolution curves and expressed as a percent of the area of the rectangle described by 100% dissolution at the same time. The percentage dissolution efficiency (DE %) was calculated by Eq. 4.

$$DE = \left[\frac{\int_{t_1}^{t_2} y * dt}{y_{100}(t_2 - t_1)} \right] \times 100 \qquad (4)$$

Where y is the percentage dissolved product. DE is the area under the dissolution curve between time point's t_1 and t_2 and it represents the maximum percentage dissolution, y100 is 100% drug dissolved over the same period.

Results and discussion

Determination of raloxifene in SBECD complex

RAL-SBECD complex was prepared in the molar ratio of 1:1. The content of RAL in the complex was 65% (w/w) and % yield was 95%.

Phase solubility studies

The main aim of this investigation was to explore the ability of SBECD to improve RAL solubility and dissolution and thereby potentiate its therapeutic activity in cancer chemotherapy. In this study, we investigated cyclodextrin inclusion complexation as a strategy to enhance RAL solubility. Freeze-drying was adopted in cyclodextrin preparation. Figure 1 presents the phase solubility diagram of RAL and SBECD in distilled water at 37±0.5°C. The increase in solubility of RAL as a function of the CD concentrations is due inclusion complex formation.[19] However, there may be other interactions involved, such as aggregation of cyclodextrins and their complexes into water soluble aggregates that are capable of solubilizing water insoluble drugs via noninclusion complexation or micelle-like structure. The coefficient of determination (R^2) values of the phase solubility diagram with SBECD was <0.990; therefore, the diagram is classified as AL-type curve.[23] The calculated stability constant of the binary system of RAL with SBECD was 753M^{-1}, suggesting that a favorable interaction generally occurs in the RAL and SBECD association constants ranging from 50 M^{-1} to 2000 M^{-1}.[24]
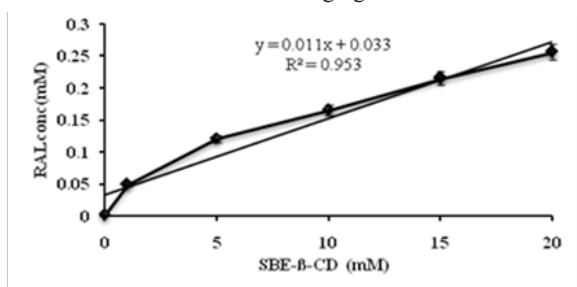

Figure 1 Phase solubility diagram of RAL with cyclodextrin in distilled water at 37±0.5°C.

Molecular docking study

The free energies of the complex formation from β-CD and SBECD were obtained by theoretical calculation. According to the energy calculation, RAL exhibited -64.19 Kcal/mol binding energy with SBECD. It is 20.33 Kcal/mol higher than RAL complex formation with β-CD (-43.86 Kcal/mol). The large binding energy of RAL clearly indicates the existence of more interactions with the SBECD molecule. This is due to RAL molecular structure, which consists of two fused ring system. RAL forms strong hydrophobic interactions with the extended sulfobutyl chains and penetrates deep inside SBECD cavity (Figure 2a) to form RAL-SBECD complex. However, these interactions are absent in RAL-β-CD complex leading to its weaker complex formation (Figure 2b).

Characterization

FTIR: FT-IR spectroscopy assessed the interaction of CD and RAL in the complex, since complexation results in shifts or changes in the absorption spectrum of RAL. Figure 3 presents the FT-IR spectra

of RAL, SBECD, physical mixture, and RAL-SBECD complex. The spectra of pure RAL (Figure 3a presented characteristic peaks corresponding to C=O and -C-O-C- stretching, -S- benzothiofuran, and benzene ring at 1642.25cm^{-1}, 1596cm^{-1}, 1466.91cm^{-1} and 905cm^{-1}, respectively. The FTIR spectra of SBECD (Figure 3b) displayed peak of –OH str at 3436cm^{-1}. All the peaks of RAL and SBECD were present in the physical mixture of RAL and SBECD (Figure 3c) However, several RAL peaks were either absent or diminished in FTIR spectra of RAL-SBECD complex (Figure 3d), indicating interaction leading to inclusion complex formation.
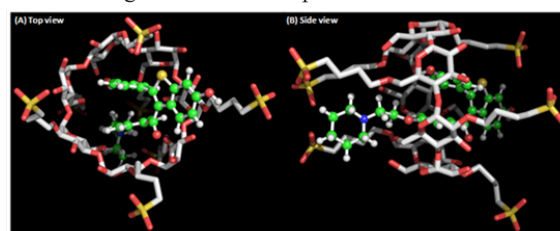

Figure 2 The complex of sulphobutyl ether β cyclodextrin (white stick) with raloxifene (ball and stick). (B) Raloxifene makes strong hydrophobic interactions with sulphobutyl ether β cyclodextrin by penetrating deep into the cavity.

PXRD: To examine the medium and long-range ordering of materials, powder XRD is the most widely employed technique. The powder XRD pattern of the RAL-SBECD complex is assumed to be distinct from that of the superposition of each of the components when a true complex is formed. The powder XRD pattern of RAL, SBECD, physical mixture and RAL-SBECD complex is presented in Figure 3b. Figure 3a presents RAL diffraction pattern where characteristic sharp crystalline peaks are present at 13°(2θ), 14°(2θ), 16°(2θ), 20.5°(2θ), 21.3°(2θ), 22.8°(2θ), and 23.1°(2θ). This pattern confirms the crystallinity of free RAL. The diffraction pattern of SBECD (Figure 3b) displays a hallow pattern indicating its amorphous nature. Sharp characteristic peaks of RAL at 13°(2θ), 14°(2θ), and 16°(2θ) were comparatively less in physical mixture (Figure 3c). However, in case of RAL-SBECD complex, no such pattern was obtained. This difference can be attributed to inclusion of RAL within the SBECD cavity. This further indicates the change in the environment of RAL and SBECD and hence confirming inclusion complex formation. This finding confirms the formation of a new kind of amorphous material. Similar results have been reported after inclusion complex formation.[25]
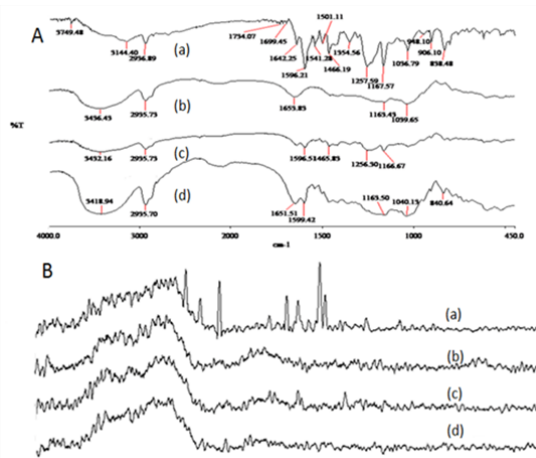

Figure 3A FTIR spectra from top to bottom a) RAL b) SBECD c) Physical mixture d) RAL- SBECD complex and B) PXRD pattern of a) pure RAL b) SBECD c) Physical mixture d) RAL- SBECD complex.

SEM: SEM has been widely employed for examination of surface morphology. Supporting evidence of RAL-SBECD complexation was obtained from SEM. Figures 4a–4d illustrate the SEM microphotographs of pure RAL, SBECD, physical mixture and RAL-SBECD complex, respectively. Typical crystals of RAL exhibited irregular shapes of varying size (Figure 4a) with adherence of small particles onto the larger ones. The SBECD particles were spherical with shriveled surface (Figure 4b). RAL-SBECD complex exhibited a remarkable and drastic change in the morphology and size (Figure 4d). The complexes were spherical with a complete disappearance of the original morphology of the individual components, confirming the interaction of RAL with SBECD and formation of inclusion complex by freeze drying.
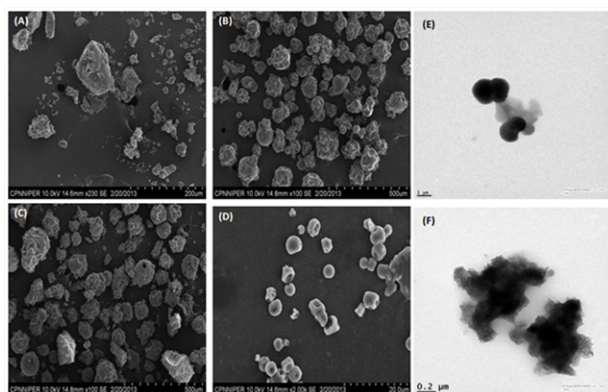

Figure 4 SEM Photomicrographs of A) free RAL, B) SBECD, C) Physical mixture, D) RAL- SBECD complex, E & F) TEM images of complex.

TEM: TEM analysis helps visually examine the surface texture and size of RAL-SBECD in water. Figure 4e & 4f present the TEM images. RAL-SBECD complex particles are in the nano-range with average size about 100-200nm. Nanoparticles of encapsulated hydrophobic drug have been reported by several research groups.[26,27] Formation of nanoparticles from preformed inclusion complexes of the anticancer drug RAL and SBECD is a successful strategy to enhance drug loading in nanoparticles. TEM results confirm the ability of CD to form an effective carrier of hydrophobic drugs.

HSM: Hot stage microscopy is a sensitive technology to detect crystallinity by occurrence of birefringence in presence of cross polarized light. Figure 5a presents the birefringence pattern of the RAL which is a characteristic of crystalline compounds. In contrast, birefringence was not present in RAL-SBECD complex indicating its amorphous nature (Figure 5b). Similarly, melting phenomena of RAL were observed, confirming its crystalline nature (Figure 5c) which was non-existent in the complex (Figure 5d) thus confirming its nature as observed by PXRD results.

NMR: To study the inclusion chemistry of complex in solution, NMR spectroscopy is a powerful technique. Change in the chemical shift values of the compound provides information about inclusion complex formation. The chemical shifts of the hydrogen atoms in the interior of the CD cavity (H^3 and H^5) become shielded and generally show a significant upfield shift in presence of a guest molecule, whereas the hydrogen atoms on the outer surface (H^1, H^2, and H^4) are not affected or experience only a marginal shift upon Complexation.[28,29] Several authors reported shielding of H^3 and H^5 protons of β and chemically modified cyclodextrin due to ring constraint because of perpendicular positioning of drugs aromatic ring within the cyclodextrin molecule cavity.[30,31]

To investigate the possible inclusion mode of RAL and SBECD in the inclusion complex formation compared the NMR spectra of RAL, SBECD and RAL-SBECD complex. Figure 6 presents the NMR spectra of RAL, SBECD and the complex. The protons of RAL exhibit distinct changes in the RAL-SBECD complex, indicating RAL is present within the cavity (Table 1).
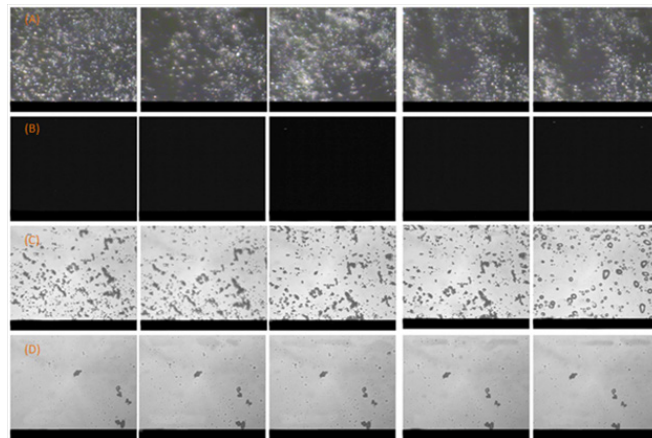

Figure 5 Micrographs of A) free RAL in cross polarized light B) Micrographs of RAL- SBECD complex in cross polarized light C) Micrographs of free RAL in ordinary light D) Micrographs of RAL- SBECD complex in ordinary light.
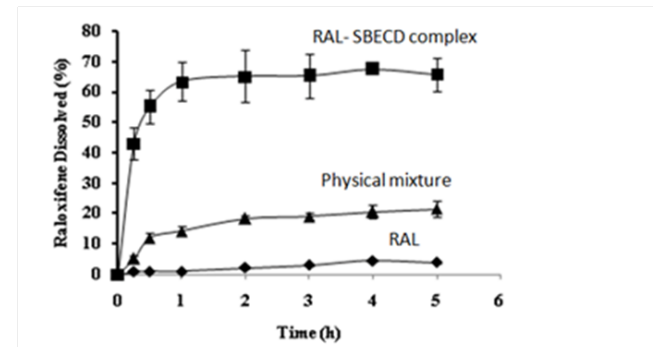

Figure 6 *In vitro* dissolution test of RAL, physical mixture and RAL- SBECD complex in phosphate buffer (pH-6.8) at 37°C. These data indicate that only 3% RAL is released at 5h compared to RAL- SBECD complex which releases significantly (P<0.05) higher ~70% drug in the same time interval.

Table 1 Changes in chemical shift values after complex formation

Protons	δ_1 ppm of RAL	δ ppm of RAL-SBECD complex	$\delta_1 - \delta_2$
H^4	7.7422	7.7388	0.0034
H^5	7.1912	7.2047	-0.0135
H^7	7.2906	7.215	0.0756
H^{13}	7.7201	7.7166	0.0035
H^{14}	6.89245	6.9025	-0.0101
H^{17}	4.2	4.248	-0.048
H^{18}	2.9584	3.05	-0.0916
H^{20}	2.7373	2.8724	-0.1351
H^{21}	1.696	1.725	-0.029
H^{22}	1.539	1.5502	-0.0112
$H^{2'}$	7.44505	7.47985	-0.0348
$H^{3'}$	6.6489	6.662	-0.0131

Determination of solubility and dissolution testing: Solubility study was conducted to investigate the effect of complexation of

RAL-SBECD complex. We observed a significant (P<0.05) solubility enhancement of RAL in the complex (0.9 versus 7×10^{-4} mg/ml) in comparison to pure RAL. Thus, solubility of RAL increased several fold by complexation with SBECD. Although, in theory, solubility determination is of important, but in practice, dissolution test is a true reflection of solubility changes.[32] Figure 7 presents the dissolution profiles of RAL-SBECD complex in phosphate buffer (pH-6.8). There was a significant (P<0.05) enhancement in the dissolution of the complex (~70% versus 3 % of RAL) at 5 h, while 12% drug was released from the physical mixture. Thus, solubilization by SBECD complex formation enhanced RAL dissolution. Poor dissolution can be attributed to RAL hydrophobic nature, which prevents wetting in the dissolution medium. Hence, RAL dissolution was increased when physically mixed with SBECD due to a combination of local solubilization effect of the CD operating in the microenvironment of the drug, or the hydrodynamic layer formation of SBECD particles over the drug in the early stage of the dissolution process, since SBECD dissolves in a short time. The increase in the drug release from the physical mixture could be to a lesser extent, to the reduction in the interfacial tension between water insoluble drug and dissolution medium by the CD, thus improving the wettability and dissolution of the drug.[33] RAL-SBECD complex exhibited a marked increase in the RAL dissolution, exhibiting almost ~70% of RAL dissolution in 5h due to formation of soluble inclusion complex of the drug with SBECD and the high energetic amorphous state or reduction of crystallinity following complexation. This is confirmed by the dissolution efficiency data presented in Table 2. Over 50-fold enhancement in dissolution efficiency was observed at fifteen minutes (t_{15}). Similar enhancement was observed at thirty minutes (t_{30}) and one hour (t_1), thus confirming the efficiency of SDECD complex in enhancing RAL dissolution.

Table 2 % Dissolution efficiency of RAL, Physical mixture and RAL- SBECD complex

% DE	RAL	Physical mixture	RAL-SBECD complex
$t_{0.25}$	0.35	2.15	17.56
$t_{0.5}$	0.668	5.5	34.64
t_1	0.824	9.33	46.48
t_2	1.194	12.77	54.88
t_3	1.658	14.74	58.01
t_4	3.133	15.9	59.01
t_5	3.353	17	61.02

Conclusion

This study was undertaken to investigate RAL-SBECD inclusion complexation by experimental and molecular modeling studies and impact of complexation on RAL solubility and dissolution profile. Freeze drying was adopted in the complex preparation. The complexes were prepared by freeze drying. Formation of complex was confirmed by FTIR, PXRD, SEM, NMR, HSM and TEM studies. RAL-SBECD complex significantly increased its solubility, dissolution rate and dissolution efficiency. Both experimental and molecular modeling studies demonstrated the superior encapsulation of RAL in SBECD. Hence, our results confirm SBECD forms stable inclusion complex with BCS Class II drugs, exemplified by RAL, with ease resulting in its enhanced solubility profile.

Conflicts of interest

The authors declare there is no conflict of interests.

References

1. Pabreja K, Dua K. Comparative evaluation of in situ intestinal absorption of aceclofenac from solid dispersions, beta–cyclodextrin complexes and coprecipitates in rats. *Bull Pharm Res*. 2011;1(1):26–30.

2. Chuah AM, Jacob B, Jie Z, et al. Enhanced bioavailability and bioefficacy of an amorphous solid dispersion of curcumin. *Food Chem*. 2014;156:227–233.

3. Pabari RM, Jamil A, Kelly Z. Fast disintegrating crystalline solid dispersions of simvastatin for incorporation into orodispersible tablets. *Int J Pharm Invest*. 2014;4(2):51–59.

4. Semalty A, Tanwar YS, Semalty M. Preparation and characterization of cyclodextrin inclusion complex of naringenin and critical comparison with phospholipid complexation for improving solubility and dissolution. *J Therm Anal Calor*. 2013;115(3):2471–2478.

5. Singh C, Bhatt TD, Gill MS, et al. Novel rifampicin–phospholipid complex for tubercular therapy:synthesis, physicochemical characterization and in–vivo evaluation. *Int J Pharm*. 2014;460(1–2):220–227.

6. Maiti K, Mukherjee K, Gantait A, et al. Curcumin–phospholipid complex:Preparation, therapeutic evaluation and pharmacokinetic study in rats. *Int J Pharm*. 2007;330(1–2):155–163.

7. Silva F, Figueiras A, Gallardo E, et al. Strategies to improve the solubility and stability of stilbene antioxidants:a comparative study between cyclodextrins and bile acids. *Food Chem*. 2014;145:115–125.

8. Rawat S, Jain SK. Solubility enhancement of celecoxib using beta–cyclodextrin inclusion complexes. *Eur J Pharm Biopharm*. 20040;57(2):263–267.

9. Reddy MN, Rehana T, Ramakrishna S, et al. Beta–cyclodextrin complexes of celecoxib:molecular–modeling, characterization, and dissolution studies. *AAPS J*. 2004;6(1):68–76.

10. Chowdary KPR, Srinivas SV. Influence of hydrophilic polymers on celecoxib complexation with hydroxypropyl beta–cyclodextrin. *AAPS PharmSciTech*. 2006;7(3):79.

11. Chowdary K, Srinivas SV. Effect of polyvinylpyrrolidone on complexation and dissolution rate of β– and hydroxypropyl–β–cyclodextrin complexes of celecoxib. *Indian Journal of Pharmaceutical Science*. 2006;68(5):631–634.

12. Rawat S, Jain S. Enhancement of intestinal absorption of few cox–2 inhibitors through interaction with?–cyclodextrin. *Indian Journal of Pharmaceutical Science*. 2007;69(4):529–534.

13. Nguyen TA, Liu B, Zhao J, et al. An investigation into the supramolecular structure, solubility, stability and antioxidant activity of rutin/cyclodextrin inclusion complex. *Food Chem*. 2013;136(1):186–192.

14. Wang J, Cao Y, Sun B, et al. Synthesis and Characterization of the Inclusion Complex of β–cyclodextrin and Azomethine. *Food Chem*. 2011;124(2011):1069–1075.

15. Patro NM, Sultana A, Terao K, et al. Comparison and correlation of *in vitro*, *in vivo* and in silico evaluations of alpha, beta and gamma cyclodextrin complexes of curcumin. *J Incl Phenomen Macrocycl Chem*. 2014;78(1):471–483.

16. Battani S, Pawar H, Suresh S. Evaluation of oral bioavailability and anticancer potential of raloxifene solid lipid nanoparticles. *J Nanosci Nanotech*. 2014;14(8):5638–5645.

17. Davis ME, Brewster ME (2004) Cyclodextrin–based pharmaceutics:past, present and future. Nat RevDrug Discov 3(12):1023–1035.

18. Irie T, Uekama K. Pharmaceutical applications of cyclodextrins. III. Toxicological issues and safety evaluation. *J Pharm Sci*. 1997;86(2):147–162.

19. Higuchi T, Connors KA. Modified β–Cyclodextrin Inclusion Complex to Improve the Physicochemical Properties of Albendazole. Complete *In Vitro* Evaluation and Characterization. *Adv Anal Chem Instrum*. 1965;4:117–212.

20. Jones G, Willett P, Glen RC, et al. Development and validation of a genetic algorithm for flexible docking. *J Mol Bio*. 1997;267(3):727–748.

21. Matsumoto N, Yamada M, Kurakata Y, et al. Crystal structures of open and closed forms of cyclo/maltodextrin–binding protein. *FEBS J*. 276(11):3008–3019.

22. Frisch M, Trucks G, Schlegel H, et al. Gaussian 03, revision C. Technical Support Information. 2008.

23. Arima H, Yunomae K, Miyake K, et al. Comparativestudies of the enhancing effects of cyclodextrins on the solubility and oralbioavailability of tacrolimus in rats. *J Pharm Sci*. 2001;90(6):690–701.

24. Wang DW, Ouyang CB, Liu Q, et al. Inclusion of quinestrol and 2, 6–di–O–methyl–β–cyclodextrin:Preparation, characterization, and inclusion mode. *Carbohydrate Polym*. 2013;93(2):753–760.

25. Yang R, Chen JB, Dai XY, et al. Inclusion complex of GA–13315 with cyclodextrins:preparation, characterization, inclusion mode and properties. *Carbohydrate Polym*. 2012;89(1):89–97.

26. Rajendiran N, Siva S, Saravanan J. Inclusion complexation of sulfapyridine with α– and β– cyclodextrins:spectral and molecular modeling study. *J Mol Str*. 2013;1054(2013):215–222.

27. Rajendiran N, Siva S. Inclusion complex of sulfadimethoxine with cyclodextrins:Preparation and characterization. *Carbohydrate Polym*. 2014;101:828–836.

28. Negi JS, Singh S. Spectroscopic investigation on the inclusion complex formation between amisulpride and γ–cyclodextrin. *Carbohydrate Polym*. 2013;92(2):1835–1843.

29. Chen W, Yang LJ, Ma SX, et al. Crassicauline A/β–cyclodextrin host–guest system:Preparation, characterization, inclusion mode, solubilization and stability. *Carbohydrate Polym*. 2011;84:1321–1328.

30. Ding L, He J, Huang L, Lu R. Studies on a novel modified β–cyclodextrininclusion complex. *J Mol Str*. 2012;979:122–127.

31. Yuan C, Jin Z, Xu X. Inclusion complex of astaxanthin with hydroxypropyl–β –cyclodextrin:UV, FTIR, 1H NMR and molecular modeling studies. *Carbohydrate Polym*. 2012;89:492–496.

32. Freitas MRD, Rolim LA, Soares MF, et al. Inclusion complex of methyl– β–cyclodextrin and olanzapine as potential drugdelivery system for schizophrenia. *Carbohydrate Polym*. 2012;89(4):1095–1100.

33. Badr ESM, Elkheshen SA, Ghorab MM. Inclusion complexes of tadalafil with natural and chemically modified β–cyclodextrins. I:Preparation and in–vitro evaluation. *Eur J Pharm Biopharm*. 2008;70(3):819–827.